Modulus Measurement for Prepreg-based Discontinuous Carbon Fiber/Epoxy Systems

PAOLO FERABOLI,* ELOF PEITSO AND TYLER CLEVELAND
Aeronautics & Astronautics, Seattle, WA, 98195-2400

PATRICK B. STICKLER
787 Technology Integration, The Boeing Co., Seattle, WA

ABSTRACT: The elastic modulus of discontinuous carbon fiber/epoxy laminates produced by compression molding of chopped unidirectional prepreg tape is measured by several means. Commercial applications for this type of material form already exist, such as Hexcel HexMC®. Although the average elastic modulus of this material has been shown to be as high as that of the continuous fiber quasi-isotropic benchmark, its non-homogenous nature gives rise to variations as high as 19% in the measurement by means of strain gage or extensometer. This phenomenon would be attributed to the variability of the manufacturing process, were it not for the fact that strength variation is much lower, with a maximum of 9%. In order to assess whether the variation observed is a result of the measurement technique and not an actual variation in material properties, a series of tensile tests is conducted while systematically varying strain gage length and location. The measurements are then compared relative to each other as well as to multiple extensometer readings along the length and opposite sides of the specimen. Digital image correlation (DIC) technique is used to gain further insight on the observed phenomena, and it has shown to be fundamental to obtain a full-field strain measurement, which is more repeatable than any of the traditional measurement techniques. Furthermore, DIC shows that complex strain distributions exist on the surface of the specimen, varying greatly along the width and across the length of the specimen, and these are associated to the non-homogeneous nature of the sub-structure.

KEY WORDS: discontinuous fibers, compression molding, digital image correlation, testing.

INTRODUCTION

AIRFRAME COMPONENTS FABRICATED from composite materials have traditionally been a costly alternative to aluminum construction. The primary challenge that the aerospace industry faced leading up to the Boeing 787 was to fully obtain the performance

*Author to whom correspondence should be addressed. E-mail: feraboli@aa.washington.edu
Figures 1–17 appear in color online: http://jcm.sagepub.com

0021-9983/09/19 1947–19 $10.00/0 DOI: 10.1177/0021998309343028

benefits of composite materials while dramatically lowering production costs [1,2]. Recent composite technology research and development efforts have focused on new low-cost material product forms, and automated processes that can markedly increase production efficiencies. The interest of the aerospace community for short fiber composites dates back to the 1960s and the pioneering work of Halpin, Pagano, and Kardos [3–6]. Although the lower mechanical properties of discontinuous fiber composites have traditionally limited their airframe applications, relatively large structures such as engine strut fairings have been in service for several years even in commercial transport aircraft. In order to become attractive for more significant secondary as well as primary structures, higher performance fiber, resins, and manufacturing methods are required. This study, comprised of several parts, investigates the behavior of a high-performance system that uses discontinuous carbon fiber/epoxy obtained from aerospace-grade unidirectional prepreg. Prepreg-based discontinuous systems are conducive for primary structural applications as they can be used in low-flow molding conditions, whereby minimal flow and reinforcement redistribution occurs upon molding. Commercial applications for this type of material form already exist, although using different resin systems and fiber types and lengths, under various manufacturers and brands (e.g., Quantum Lytex 4149 and Hexcel HexMC® [7,8]). The Boeing 787 Dreamliner, for example, makes use of AS4/8552 HexMC® for the window frames, as well as other secondary structural elements.

In part I of this series [9], a manufacturing technique is developed that allows for the manufacturing of randomly distributed chip-reinforced composite plates. Good manufacturing procedures show that the plate contains minimal number of voids, although resin-rich areas are inevitably present due to the flow of the resin during cure. The study shows that chip dimensions, such as aspect ratio, have a strong effect on the measured strength but a negligible effect on the modulus, which is as high as that of the continuous fiber quasi-isotropic reference value. However, noticeable variation in both modulus and strength data is reported, and it varies according to the loading conditions and specific property measured. Failure is a matrix-dominated event, which occurs by transverse chip cracking, longitudinal chip splitting, and chip disbonding, with little fiber breakage, and tensile strength is noticeably lower than a quasi-isotropic continuous baseline.

In part II [10], the chip aspect ratio is fixed at a value of 2.0 in $\times$ 0.33 in (50.8 mm $\times$ 8.4 mm), which is a good compromise between mechanical properties and manufacturing considerations. The panels are shown to be free of defects such as micro-voids or resin-starved areas. The resin system is modified to a much tougher one thereby increasing shear transfer between matrix and fibers. More extensive fiber breakage is observed, resulting in higher average tensile strengths, and lower variation (5–9%). However, the variation observed in tensile modulus measurements remains as high as 19%, while the average value is still as high as that of the continuous fiber quasi-isotropic baseline.

This part of the investigation focuses on addressing the issues behind the observed variations in elastic modulus as measured by extensometer, strain gages, and digital image correlation technique (DIC).

MATERIAL FABRICATION AND TEST SETUP

All discontinuous carbon/epoxy specimens are manufactured in the laboratory starting from T700/977 unidirectional (UD) prepreg. The system is a 350°F cure (177°C),

designated for vacuum bag, autoclave cure, and has a resin content of 40%. The detailed procedure of how the unidirectional prepreg is slit and then chopped in order to obtain the desired random chip distribution is reported in part I of the series [9]. The chip dimensions are 2.0 in long × 0.33 in wide (50.8 mm × 8.4 mm) [10]. Each specimen is shown to be defect-free via non-destructive inspections, such as pulse-echo ultrasound and pulse thermography, and via optical microscopy [9,10].

Specimens are tested using the Boeing standard test method D6-83079-61 [11] for unnotched tension (UNT), which features straight-sided rectangular specimens with dimensions 12 in × 1.5 in (305 mm × 38 mm) and nominal thickness of 0.168 in. (4.3 mm). All specimens are loaded at a rate of 0.05 in/min. (1.3 mm/min) in a two-grip hydraulic tension/compression test frame. Glass/epoxy tabs are bonded to the specimen using 3M Scotchweld film adhesive, see Figure 1.

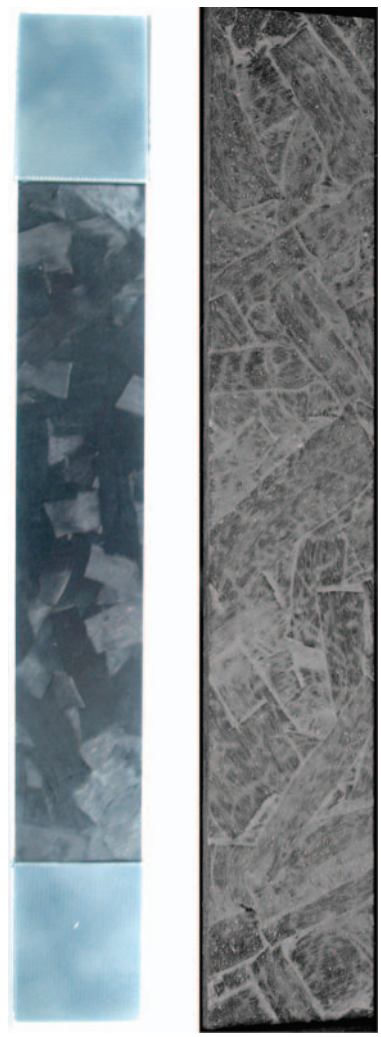

Figure 1. *Typical tensile specimen with glass/epoxy tabs (left), and close-up of the random chip surface distribution, as highlighted via ultraviolet light (right).*

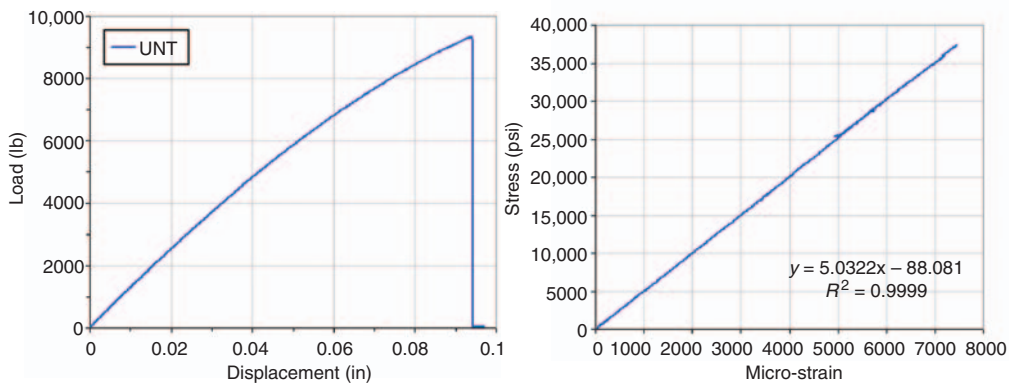

Figure 2. *Representative load–displacement (left) and stress–strain (right) curves for the UNT specimens.*

Typical load–deflection and stress–strain curves are shown in Figure 2, where the deflection is given by cross-head displacement, and the modulus is measured by a single extensometer located at mid-gage of the specimen. Figure 2 is only meant to be representative of a typical test were the specimen to be comprised of continuous tape. Given the unique nature of this material, more details on the modulus measurement techniques follow below. All specimens are loaded conservatively to 2500–3000 microstrain or approximately 3000 lb (13 344 N), in order to ensure that the behavior remains in the purely elastic region. A limited set of specimens is loaded up to failure, and it is found that the stress–strain plots remain perfectly linear up to catastrophic failure.

Each specimen is instrumented with multiple strain gages, of varying size and location, as well as an extensometer. Uniaxial strain gages used in this study include 0.125, 0.250, 0.5, 1.0, and 2.0 in (3.2, 6.3, 12.7, and 25.4 mm respectively) long gages. It should be noted that gages of length in excess of 0.5 in (12.7 mm) are less frequently used than the shorter ones, and are typically more expensive to purchase. Furthermore, the longer gages tend to be more difficult to be positioned and bonded accurately, thereby resulting in a less controlled procedure. Strain gage location is varied between mid-gage of the specimen, along its length, and across its width, and details are given in the results section as each specimen is discussed in detail. The 1.0-in gage (25.4 mm) extensometer readings are obtained in multiple locations along the specimen length and by shifting the position from one side to the other.

All modulus measurements reported in the following section are the average of three independent measurements, which are run consecutively on the same specimen and in the same fashion, after ungripping, realigning, and reloading the specimen in order to guarantee repeatability. Eleven total specimens have been tested, and Table 1 offers the details of the full test matrix.

A limited number of specimens are also loaded in the test frame while being monitored by the DIC system, VIC-3D provided by Correlated Solutions Inc. The system consists of two high-resolution cameras and an image analysis computer program capable of measuring large displacements and strains [12,13]. The specimen is typically coated with a white spray paint, and a random pattern of black speckle marks is applied to the surface to be analyzed. The photogrammetry system captures images of the deforming object at predefined intervals during the test and compares them, thereby constructing a real-time plot of the deformation. This system can provide unique insight in the full-field strain state of the specimens due to its non-contact and non-local nature.

Table 1. Global test matrix for this study.

Specimen no.	Total no. gages	Strain gage description	Extensometer description	High modulus (Msi)	Low modulus (Msi)	Avg modulus (Msi)	CoV (%)
1	3	1 × 0.5 in front center 1 × 1.0 in front center 1 × 2.0 in front center	1 × center	9.26	6.76	7.52	16
2	4	2 × 0.25 in. front center 1 × 1.0 in front back 1 × 2.0 in front back	1 × center	6.02	3.75	4.6	18
3	6	3 × 0.5 in front center 3 × 1.0 in back center	1 × center	6.89	4.82	5.78	14
4	6	3 × 0.5 in front center 3 × 0.5 in back center	2 × center	7.12	5.08	5.93	12
5	6	3 × 1.0 in front center 3 × 1.0 in back center	2 × center	7.09	5.04	5.82	13
6	12	2 × 0.5 in front top 2 × 0.5 in front center 2 × 0.5 in front bottom 2 × 0.5 in back top 2 × 0.5 in back center 2 × 0.5 in back bottom	1 × top, center, bottom	7.68	4.82	6.09	14
7	12	1 × 0.5 in front top 1 × 1.0 in front top 1 × 0.5 in front center 1 × 1.0 in front center 1 × 0.5 in front bottom 1 × 1.0 in front bottom 1 × 0.5 in back top 1 × 1.0 in back top 1 × 0.5 in back center 1 × 1.0 in back center 1 × 0.5 in back bottom 1 × 1.0 in back bottom	1 × center	7.56	4.72	6.11	12
8	N/a	DIC	2 × top 2 × center 2 × bottom	7.01	4.37	5.69	13
9	N/a	DIC	2 × top 2 × center 2 × bottom	7.17	4.64	5.57	12
10	N/a	DIC	2 × top 2 × center 2 × bottom	7.97	3.02	5.92	19
11	8	2 × 0.125 in on 0° front top 2 × 0.125 in on 90° front top 1 × 0.125 in on 90° back top 1 × 0.125 in on 45° front bottom 1 × 0.125 in on 90° front bottom 1 × 0.125 in on 90° back bottom	3 × top 2 × bottom	8.73	5.98	7.12	14
AVG TOT	–	77 × 3 readings	–	9.26	4.33	6.26	17

RESULTS

Specimen configurations and results are summarized in Table 1. It should be noted that of all specimens tested, the average modulus measured varies between 4.60 and 7.52 Msi (31.7 and 51.8 GPa), with an average of 6.1 Msi (42.0 GPa), and the coefficient of variation (CoV) lies between 12 and 18%. As a reference, the continuous fiber carbon/epoxy tape T700/977 prepreg modulus for a quasi-isotropic $[+45/0/-45/90]_{2s}$ lay-up is 6.5 Msi (44.8 GPa). Due to the particular nature of this study, which employs a limited set of specimens that have been highly instrumented, each specimen and related instrumentation details is discussed a separate paragraph. The values reported in Figures 3–15 represent average modulus measurements.

Specimen 1 is tested to study whether it is necessary to employ special length strain gages or if it is acceptable to employ conventional ones. Three strain gages are positioned in the center of the specimen gage section and on its front face, having lengths of 0.5, 1.0, and 2.0 in (12.7, 25.4, and 50.8 mm) respectively, see Figure 3. The extensometer is located in the same position and the measurements are collected simultaneously. As it can be seen, it appears that the extensometer, the 2.0-in gage (50.8 mm) and the 0.5-in (12.7 mm) gage all provide modulus measurements around 7.0 Msi (48.3 GPa), while the 1.0-in gage (25.4 mm) appears to give excessively high readings (9.26 Msi or 63.8 GPa). It should be recalled that each value reported is the average of three independent measurements to ensure repeatability. It is suggested that the specimen may be unevenly loaded due to a misalignment, while it appears that the length of the gage may not be as influent as originally thought.

Specimen 2 is tested to isolate possible eccentricities in the specimen loading and to corroborate the observations proposed for Specimen 1. Four strain gages are positioned in

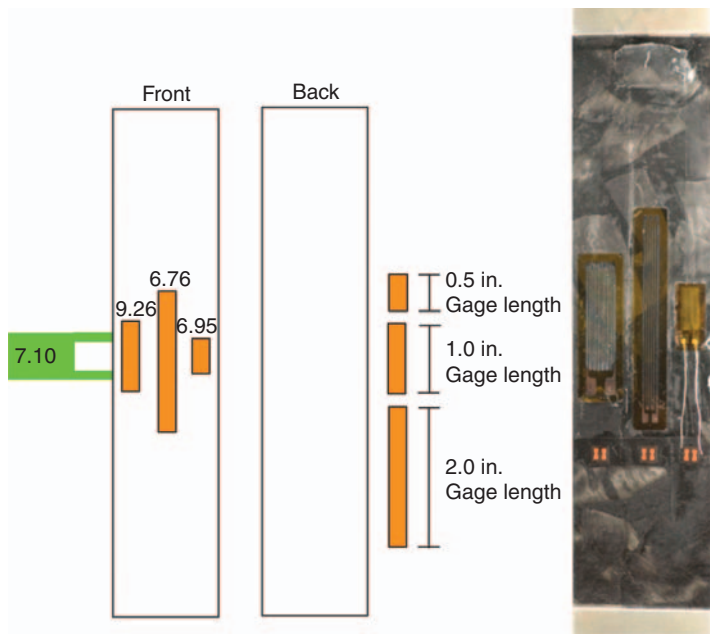

Figure 3. *Specimen 1 features 1.0, 2.0, 0.5 in. (25.4, 50.8, 12.7 mm) long strain gages in the front center gage section.*

the center of the specimen gage section, two on its front face and two on its back face. The former have lengths of 1.0 and 2.0 in (25.4 and 50.8 mm) respectively, while the latter are 0.25 in both (6.3 mm), see Figure 4. The extensometer is located in the same position and the measurements are collected simultaneously. As it can be seen from Figure 4, it appears that the extensometer, the 1.0-in and the 2.0-in gages (25.4 and 50.8 mm respectively) all provide modulus measurements in the range of 4.4 Msi (30.3 GPa). The smaller gages on

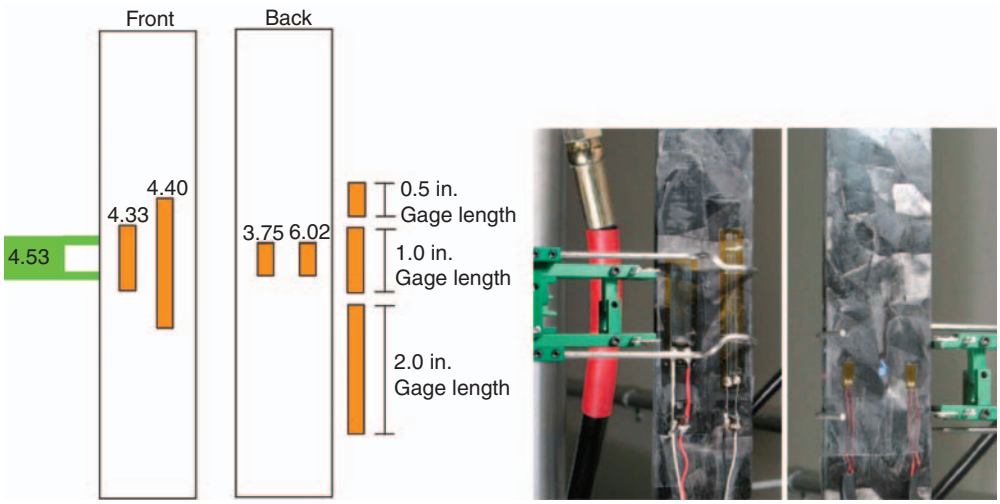

Figure 4. *Specimen 2 features a 1.0 (25.4 mm) and a 2.0 in. (50.8 mm) gage in the center front section, and two 0.25 in. (6.3 mm) gages in the center back section.*

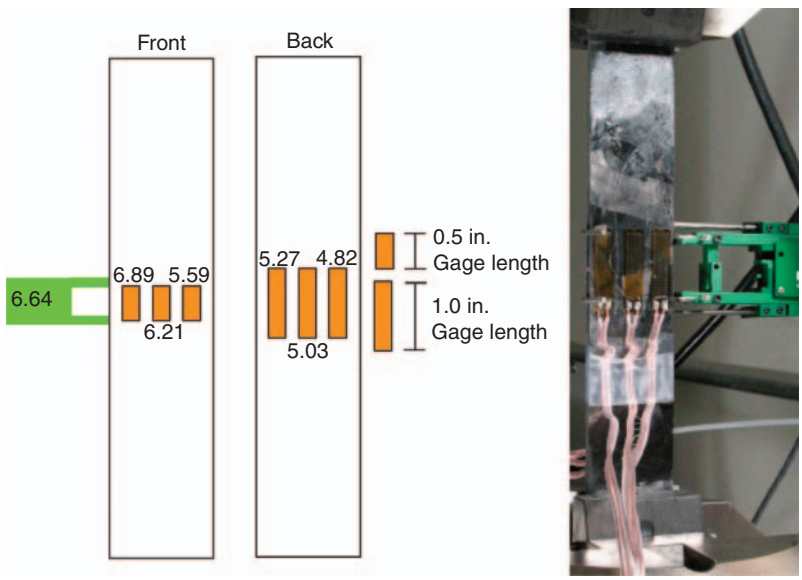

Figure 5. *Specimen 3 features three 0.5 in. (12.7 mm) gages in the front center section, and three 1.0 in. (25.4 mm) gages in the back center section.*

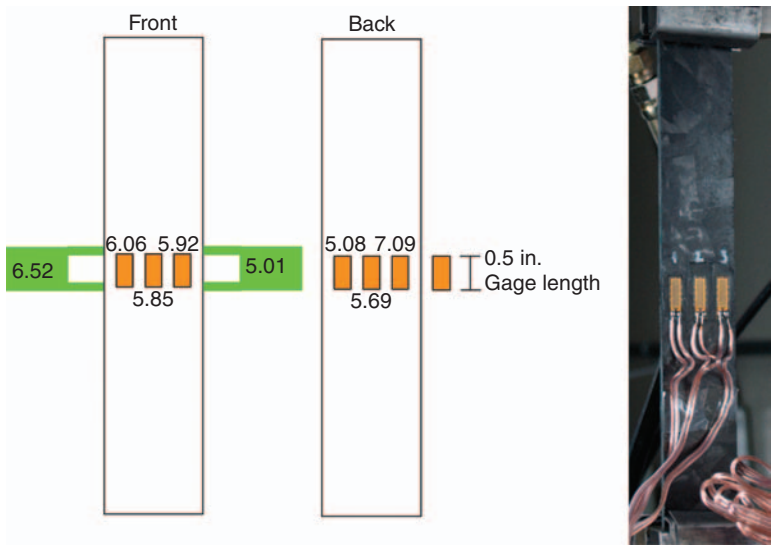

Figure 6. *Specimen 4 features six 0.5 in. (12.7 mm) gages in the front and back center section.*

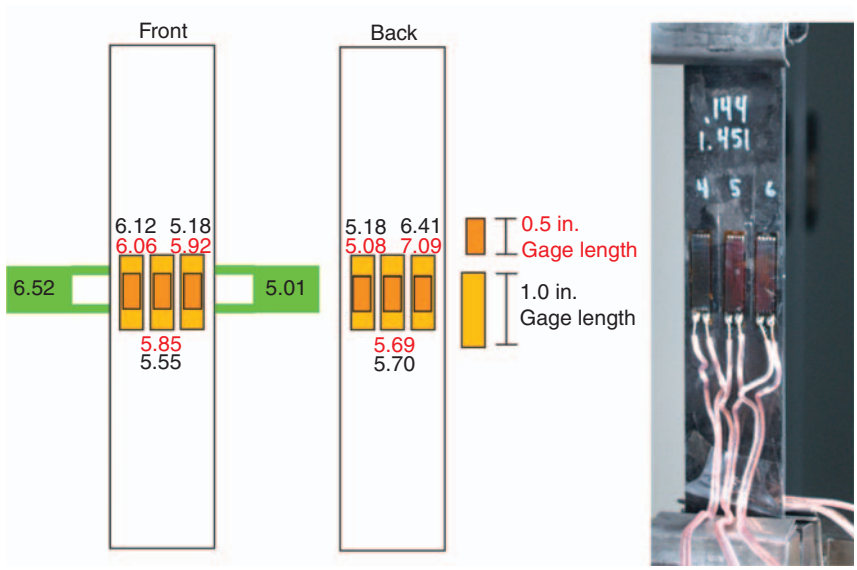

Figure 7. *Specimen 5 (same as Specimen 4) features six 1.0 in. (25.4 mm) gages in the front and back center sections, superimposed to the previous six 0.5 in. (12.7 mm) gages.*

the back face appear to provide completely different responses, one slightly lower (3.75 Msi or 25.8 GPa), while the other much higher (6.02 Msi or 41.5 GPa). The variation across the width as high as 2.3 Msi (15.8 GPa) is thought to be an erroneous reading, whereby the 0.25-in (6.3 mm) gages may be too small for this material form, but concerns also arise about potential eccentricities between front and back faces.

Specimen 3 is tested to identify the variation across the width using the same gage length, using two different strain gage lengths. Three 0.5-in (12.7 mm) gages on the front face and

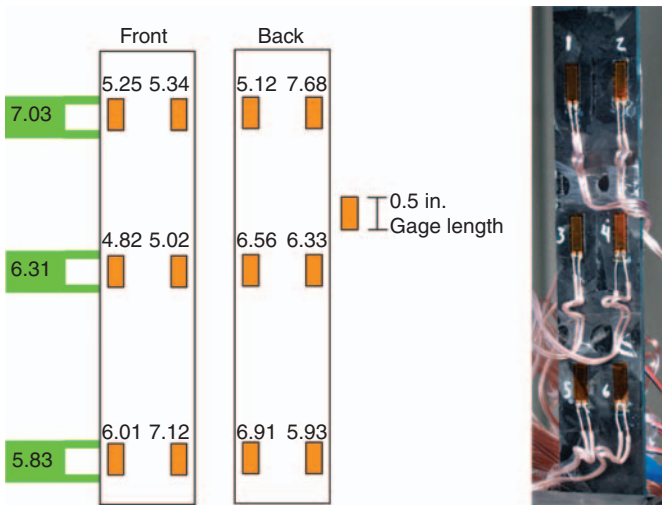

Figure 8. *Specimen 6 features twelve 0.5 in. (12.7 mm) gages in the front and back sections, in the top, center, and bottom portions of the specimen.*

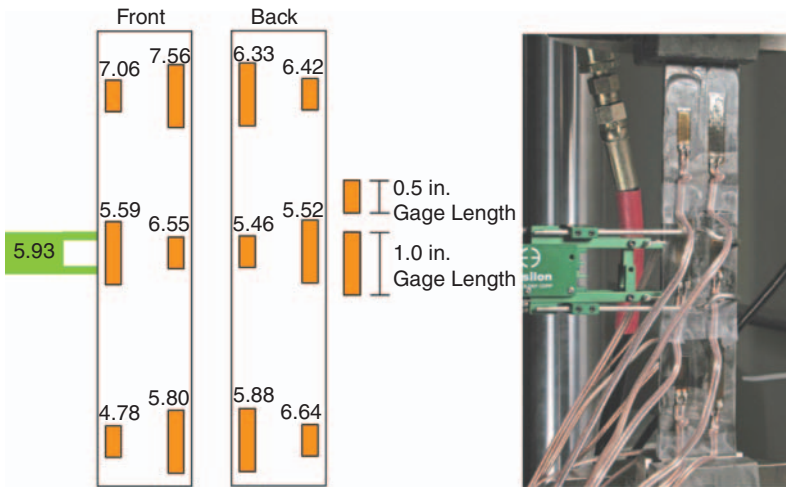

Figure 9. *Specimen 7 features six 0.5 in. (12.7 mm) gages and six 1.0 in. (25.4 mm) gages alternating in the front and back sections, in the top, center, and bottom portions of the specimen.*

three 1.0-in (25.4 mm) gages on the back face are located in the center of the specimen gage section, where the extensometer is also positioned, Figure 5. It can be seen that on the front face the modulus measurements provided by the 0.5-in gages (112.7 mm) averages 6.23 Msi (42.9 GPa), with the extensometer around 6.6 Msi (45.5 GPa). On the other hand, on the back face, the 1.0-in gages supply values that are consistently lower at an average of 5.04 Msi (34.7 GPa). This discrepancy could be attributed to either gage length or an eccentricity in the specimen loading, although the measurements across the width exhibit variations as high as 1.3 Msi (8.9 GPa), consistently with observations on specimen 2.

Specimen 4 is very similar to the previous one, with the exception that it attempts to isolate the strain gage length variable by testing six 0.5-in (12.7 mm) gages. Three on the

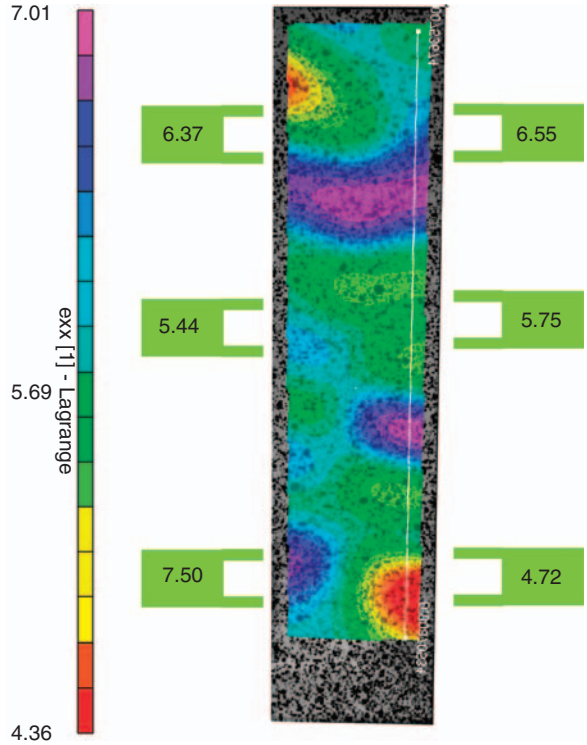

Figure 10. *Specimen 8 modulus contour plot via digital image correlation technique.*

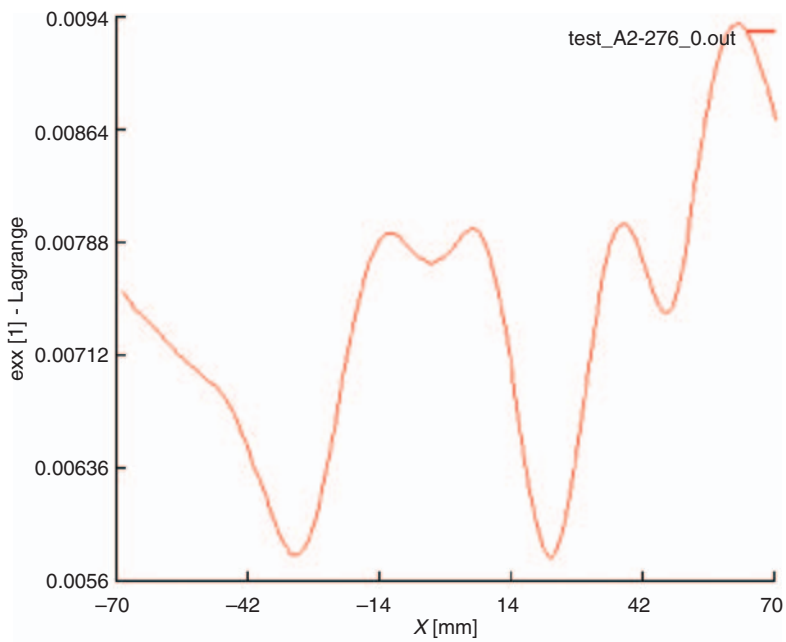

Figure 11. *Variation of longitudinal strain along the path defined in Figure 10.*

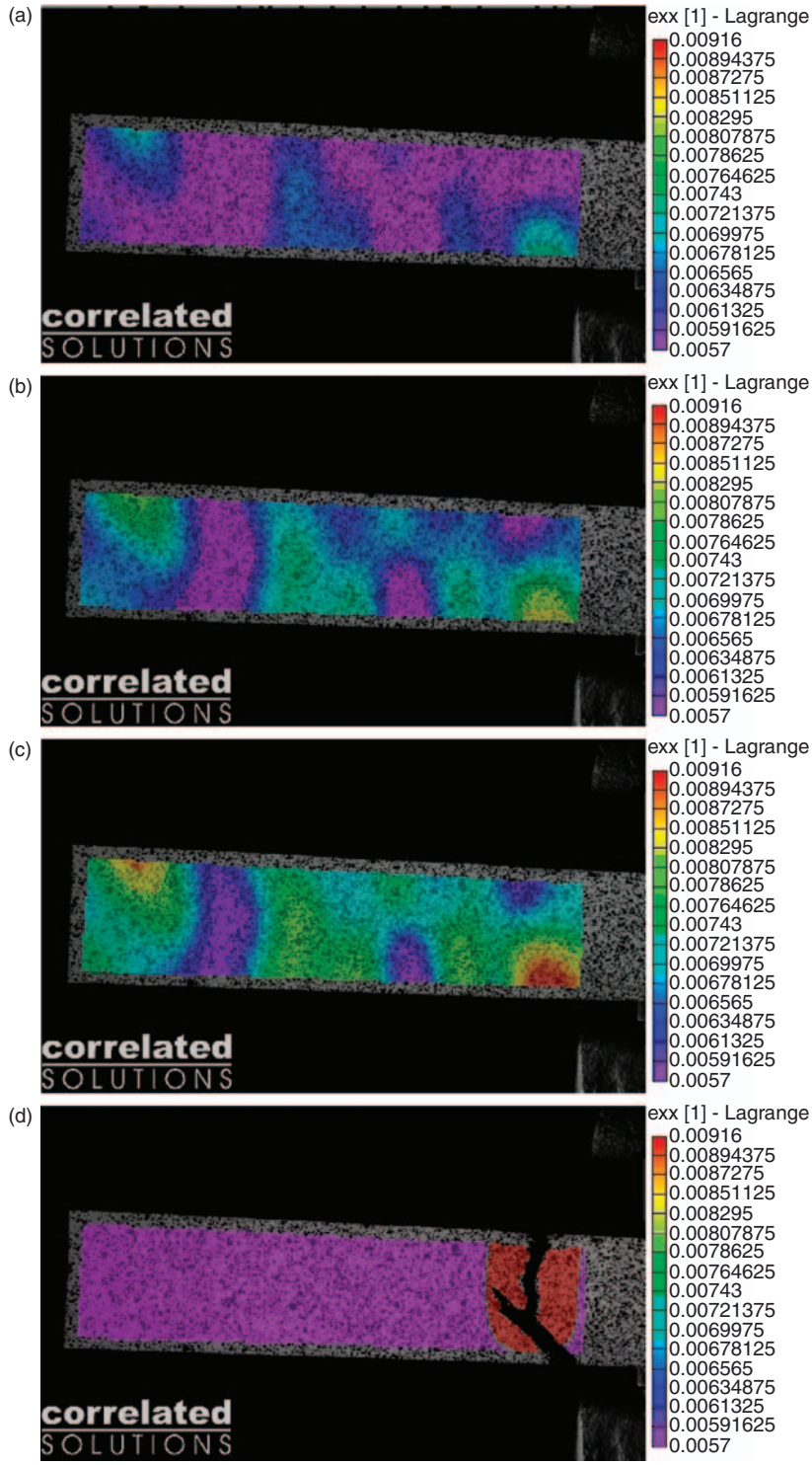

Figure 12. *(a–d) Evolution of the DIC axial strain contours for specimen 8, up to final rupture.*

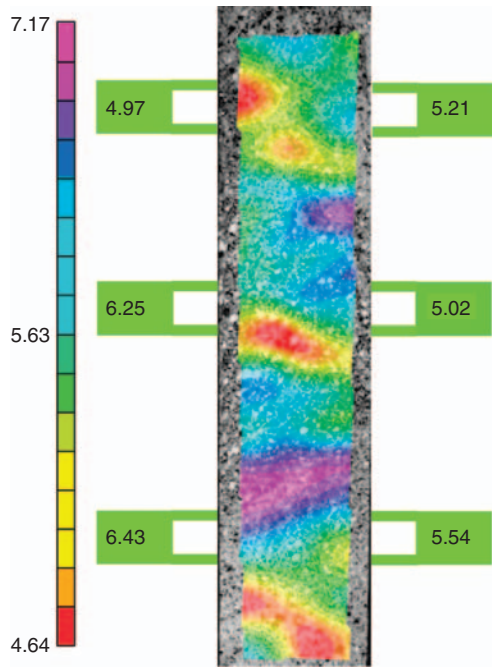

Figure 13. *Specimen 9, or second DIC specimen.*

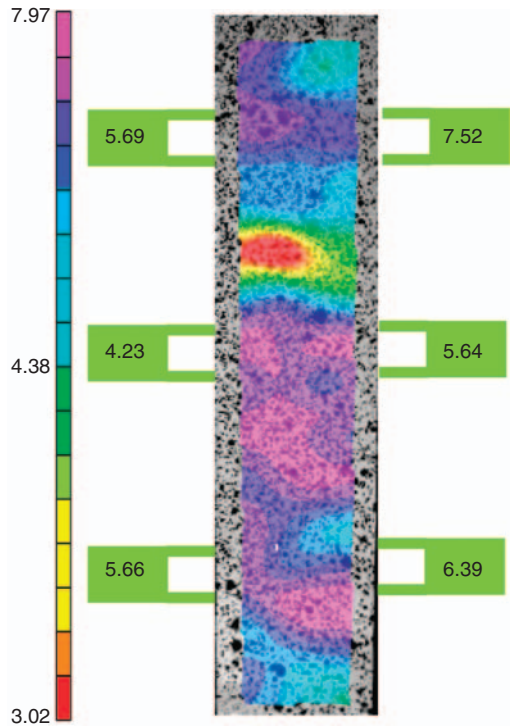

Figure 14. *Specimen 10, or third DIC specimen.*

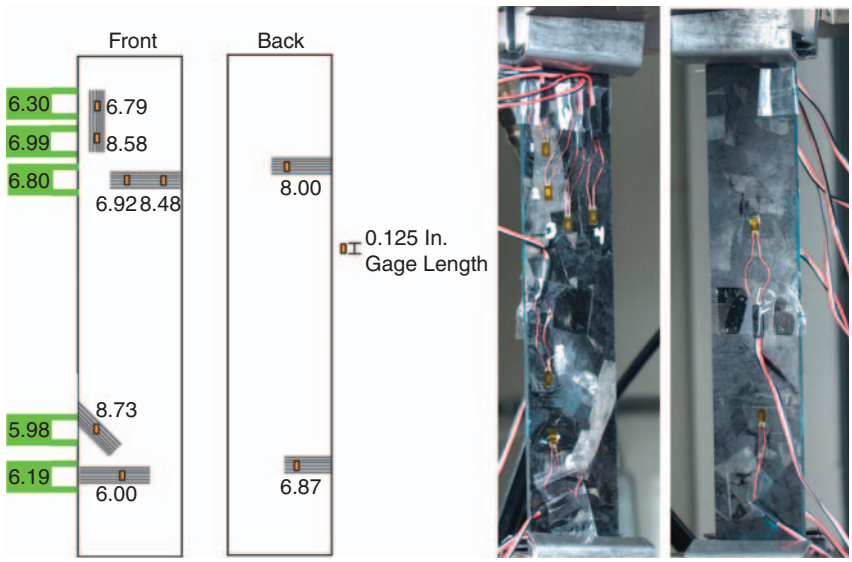

Figure 15. *Specimen 11 features eight 0.25 in. (6.3 mm) strain gages located over individual chips oriented at 0°, 90°, and 45°.*

front face and three on the back face, located in the center of the specimen gage section, where the extensometer is also positioned, Figure 6. From the results, the first observation that can be made is that the two extensometer readings, with the device positioned first on the right side and then on the left side, provide a large variation in measurements: 5.08 Msi vs. 6.52 Msi (35.0 GPa vs. 44.9 GPa). It should be reminded that these results are the averages of three different runs, obtained after removing and regripping the specimen. This in turn suggests that even positioning the extensometer on one side instead of another can lead to different measurements, an atypical finding for traditional aerospace composites. A second observation is that while on the front face the three gages yield similar results that range between 5.89 and 6.13 Msi (40.6 and 42.3 GPa respectively), the back side yields results that vary between 5.09 and 7.12 Msi (35.1 and 49.1 GPa). The specimen appears to be well aligned as front and rear measurements do not vary because of an eccentricity in the loading, but large strain gradients on the surface of the specimen appear to be present, which neither the 1.0-in (25.4 mm) extensometer nor the 0.5 in (12.7 mm) gages can average out. This finding requires careful investigation.

The six 0.5-in (12.7 mm) strain gages of specimen 4 are carefully removed with a razor blade, the surface is lightly abraded, cleaned, and dried prior to bonding six new gages. The newly obtained specimen 5 features six 1.0-in (25.4 mm) gages that are carefully placed in the exact same locations as the previous ones. Readings from the 1.0-in (25.4 mm) gages are placed right next to the previous 0.5-in (12.7 mm) ones for direct comparison, Figure 7. Results show that, in at least four of the six readings, the smaller gages yield virtually identical results as the longer ones. For the other two gages, the larger gages yield approximately 10% lower modulus measurements than the smaller gages. In general however it is fair to conclude that 0.5- (12.7 mm) and 1.0-in. (25.4 mm) gages yield very similar readings. As expected, the two extensometers readings are nearly identical to the ones of specimen 4 (Figure 6), but they are not identical on the opposing sides of the specimen.

In order to better quantify the variation of strain on the specimen surface, specimen 6 is tested using a total of twelve 0.5-in (12.7 mm) gages, of which six are on the front face, and six are on the back face. These are bonded in sets of two next to each other along the length of the specimen, from top to center to bottom, Figure 8. Results show a large variation in strain both across the width and along the length of the specimen. Extensometer readings at top, center and bottom, all on the same side of the specimen, yield measurements from 5.83 to 7.03 Msi (40.2 to 48.5 GPa). Similar variation can be observed from the measures of various gages down the length of the specimen. Across the width, each set of gages is spaced by only 0.5 in (12.7 mm), and yet variations as high as 5.12–7.68 Msi (35.3 to 53.0 GPa) are seen locally. A source of concern is that the extensometer readings at approximately the same position along the specimen length as the strain gages yield results that are far from the averaged measurements of those strain gages, hence the interaction in strain fields between chips through thickness, along length and across the width is all but predictable.

Similar to the previous specimen, specimen 7 is tested to verify the observed anomalies in surface strain distributions. This specimen contains twelve gages positioned in the same fashion as the previous one, except that each pair of strain gages contains one 0.5-in (12.7 mm) gage and one 1.0-in (25.4 mm) gage. The extensometer is placed in one location at the center of the specimen gage. The results shown in Figure 9 show a variation of 1.0 Msi (6.9 GPa) across the width, but a much greater one along the length.

The aforementioned non-uniformity in the strain field on the specimen surface is likely attributable to the non-homogeneous nature and the finite length-scale of the chip reinforcements. It becomes of interest to characterize the surface strain distributions in an attempt to correlate them with the surface chip orientations. To that extent, specimen 8 is loaded in the test frame while being monitored by the commercially available DIC system. Although the system is capable of 3D acquisitions, for the purpose of this investigation only the 2D image is reported. Six measurements with the extensometer are also performed on both sides of the specimen and at three different locations along its length, Figure 10. It should be noted that the extensometer readings on the left and right sides are relatively similar to each other on the top and center location, but the bottom measurements yield a large discrepancy at 7.50 and 4.72 Msi respectively (51.7 and 32.5 GPa). It should be noted that the control window of Figure 10 focuses on the center 6.0 in (152.4 mm) of the specimen, thus at least 2.0 in (50.8 mm) away on each side from the tabs which are 1.0 in (25.4 mm) long. The contour plot shows extremely valuable information that confirms the really high variation in surface modulus distribution, ranging from 4.37 to 7.01 Msi (30.1 to 48.3 GPa). The high and low modulus areas shown in purple or red respectively are to be considered fully removed from local stress concentrations near the grips. These hot spots appear to vary without a specific pattern along the length and across the width of the specimen, and are to be considered the source of the contrasting modulus measurements. In Figure 10 is visible a straight white line approximately 5.5 in (139.7 mm) long, which runs longitudinally along the specimen. Along this path is possible to plot the variation in longitudinal surface strain, Figure 11.From the contour data it is immediate to calculate the average full-field modulus of the material at 5.69 Msi (39.2 GPa), with a CoV of 13%. It is of interest to observe that the average value measured via DIC is relatively close to the average center readings of the extensometer.

The entire evolution of surface strain distribution is shown from the unloaded specimen up to rupture in Figure 12 (a)–(d). From Figure 12 it is evident that as the loading begins, these areas of non-uniform strain appear (a) and grow (b, c), until eventually failure

originates from the largest and strongest of the two hot spots (d). This hot spot corresponds to the area of lower modulus for the specimen, as shown in Figure 10. Other two specimens, 9 and 10, are tested elastically and then to failure using the same DIC system. The results, very similar to the ones of Figure 10, are reported in Figures 13 and 14 respectively. Maximum, minimum, average values, and CoV are reported in Table 1.

Specimen 11, the last tested, employs the smallest available gages (0.125 in or 3.2 mm), which are carefully positioned over individual chips on the surface of the specimen. Each of the eight gages is positioned on a chip of a specific orientation with respect to the longitudinal, at 0°, 90°, or 45°, Figure 15. It can be seen that in two cases, there are two strain gages located on the same chip, a 0° and a 90° chip on the front top section. Almost identically on the opposite side, there is another strain gage on a 90° chip on the back top section. Similarly there is one gage on a 90° chip on the front bottom face, and one exactly on the other side in the back bottom face. Extensometer readings are performed on the strain gage side at nearly the same longitudinal location as the strain gage itself. Several conclusions can be obtained. First, the orientation of the chip does not bear direct influence on the measured strain. This is suggested by the fact that the 0°, 90°, and 45° chips yield inconsistent measurements, and that the measurements vary also within each chip. It appears that the surface strain is the result of the whole underlying laminate meso-structure, which in turn means that the orientation of the chips through the entire thickness of the specimen dictates the surface strain behavior. Second, it is shown that local extensometer readings are once again not the average of the local strain gage readings at that same location.

To verify the validity of the methodology used throughout the study, two specimens of clearly distinct material form are tested in a similar fashion to the specimens of Figures 10, 13, and 14. For each specimen, six modulus readings along the length and on both sides are obtained with the aid of the extensometer, while full-field strain plots are obtained with the DIC system.

The first specimen, Figure 16, is a continuous fiber carbon/epoxy specimen with a bias $[+45/02/-45/03/90]_s$ lay-up, manufactured with the same prepreg mentioned above. It can be seen that extensometer readings vary from 13.06–11.55 Msi (90.0–79.6 GPa) according to location, while DIC readings vary from 13.76–11.71 (94.8–80.7 GPa). In general, while a moderate variation in measured modulus is present along the face of the specimen, possibly due to minor misalignments of the specimen in the grips and of the DIC set-up, the overall strain distribution on the surface is quite homogeneous. Furthermore, all extensometer readings are consistent with the local strain field shown by DIC.

The second specimen, Figure 17, is obtained by resin transfer molding (RTM) of chopped glass/epoxy random mat. The glass reinforcement is 1.0 in (25.4 mm) long. This material form is specifically selected to provide an alternate discontinuous fiber system for comparative purposes. Extensometer readings vary from 2.39–2.15 Msi (16.5–14.8 GPa), while DIC measurements vary from 2.48 to 2.08 Msi (17.1 to 14.3 GPa). Unlike the previous observations on chopped prepreg systems in this study (Figures 10, 13, 14), it can be seen that the overall strain distribution is very uniform, and extensometer readings are very accurate compared to DIC values. Counterintuitively, it appears that not all discontinuous fiber systems exhibit the same non-uniformity in strain field, but the results reported in this study are a characteristic trait of chopped carbon/epoxy unidirectional prepreg systems. It is possible that the large modulus variations measured in the chopped prepreg system can be attributed to the large size of the unidirectional chip, which is longer and wider than the fiber tows used in random mats, has relatively high modulus, carbon

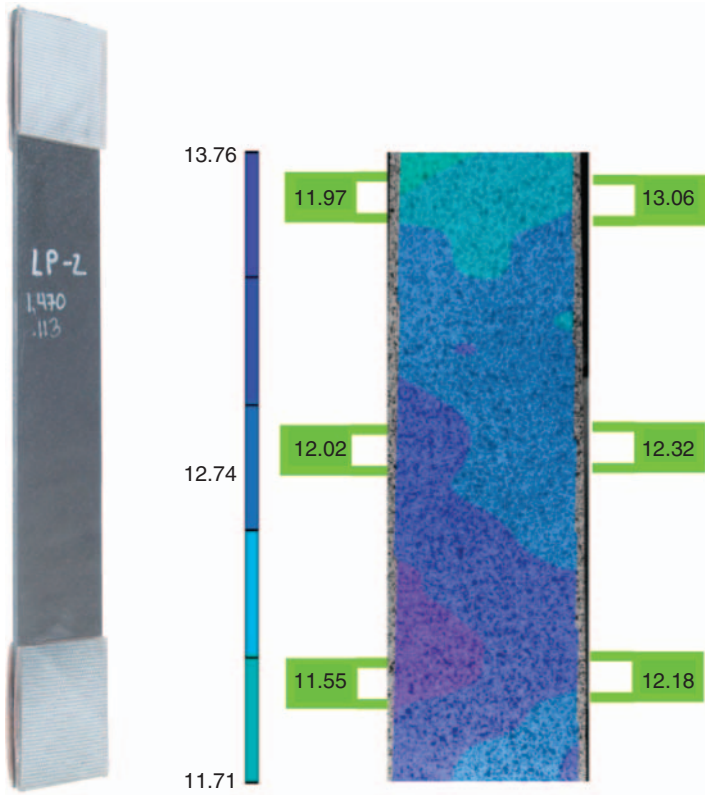

Figure 16. *Comparison DIC readings for continuous fiber carbon/epoxy prepreg specimen with* $[+45/02/-45/03/90]_s$ *lay-up.*

greater than glass, and its a straighter (or less-deformed) shape within the laminate. The reinforcing unit chip exhibits local stiffness properties that vary greatly according to chip orientation, and this in turn gives rise to measurable discontinuities in the macroscopic modulus. It is possible to hypothesize that the distribution of chips at the mesoscopic level affect the macroscopic modulus measurements more than the properties at the fiber/resin microscopic level.

DISCUSSION

Experimental results show that this material form exhibits high surface strain variations, both across the width and along the length of a typical tensile specimen. However, these are not directly related to the orientation of the surface chips, but are the result of the heterogeneous properties of the 'laminate' through its entire thickness. Measuring the actual modulus of the material becomes a difficult task from an experimental standpoint, as well as a philosophical challenge. Interestingly, the high variation in modulus values observed previously for this material form is not to be attributed to a variability in the manufacturing process, and hence a variation in specimen to specimen or batch to batch, but as variability within a single specimen due to the nature of the material substructure.

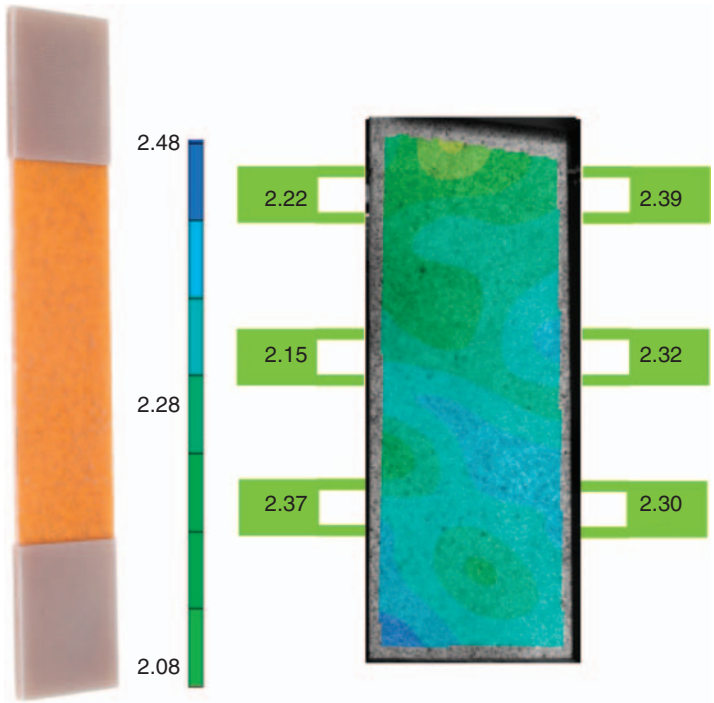

Figure 17. *Comparison DIC readings for short fiber glass/epoxy specimen obtained by RTM of dry random mat.*

From a technical standpoint, use of strain gages imposes great limitations, as their length is smaller than the dominant length scale of the material. Strain gages 0.125 and 0.250 in long (3.2 and 6.3 mm respectively) have shown to yield unacceptably high variation in modulus measurements depending on their location, and should therefore not be used for this material form. Strain gages 0.5, 1.0, and 2.0 in long (12.7, 25.4, and 50.8 mm respectively) have shown to yield nearly identical results, but have also shown to give rise to high variations in readings among multiple locations. Longer gages, typically more expensive, less readily available, and more difficult to bond should not be preferred over the smaller 0.5 in. (12.7 mm) gages. Extensometer readings, using a 1.0 in. gage (25.4 mm), have also shown to give rise to inconsistent modulus values according to their position, both along the length and on the two opposite sides of the specimen. It is therefore not recommended to rely on the readings of one extensometer alone, but to repeat the measures in at least six locations along the specimen (top, center, and bottom for both sides) and to average the results. DIC techniques have shown to give great insights in the behavior of the specimen, and provide the most comprehensive modulus measurement by averaging the full-field strain measurements over the entire gage section.

From a philosophical standpoint, it is worthy to ask the question whether the 'averaged' modulus has actually any significance other than being of qualitative or informational nature. Given the fact that these hot spots, or regions of significant strain gradients, have characteristic sizes in the range of the 0.5–1.5 in (12.7–38.1 mm), Figures 10 and 11, it may become important to assess the local state of strain rather than the global one. This is particularly true in the proximity of a fastener or fastener hole, where relative part stiffness

dictates the load sharing between mating parts. It also appears that these hot spots become stronger with increased loading, and eventually precipitate failure. It has been shown through DIC that the location of peak surface strain, hence lowest modulus, corresponds to the location of rupture.

Other considerations of importance deal with methods of analysis for these materials. Traditional analysis approaches that have been successfully used to predict the elastic response (not the strength) of discontinuous fiber composites include those of Halpin and Pagano, Mori-Tanaka and Pipes, and Wetherhold [14,15]. However, none of these methods is capable of predicting the variation in modulus observed for this material, and should only be used, at best, to predict the average modulus, based on either the microstructural constituents or the macroscopic laminate-equivalent properties. These challenges translate also in potential obstacles for the certification process, which is typically performed by test or by analysis. By test, the large variations observed may impose very conservative upper and lower bounds, and hence result in overweight designs. Similarly, in the case of certification by analysis, the variability attributed to the material may result in overly conservative allowable values, and perhaps lead to puzzling anomalies when comparing experiment and analysis predictions during limit load strain surveys of actual components.

The composite material form described in this series of studies offers excellent mechanical properties and, in particular, the elastic modulus and the open-hole strengths are within a few percent of the continuous fiber quasi-isotropic benchmark values [9,10]. In general, the modulus of the material – average of all measurements for all specimens 77 values between gages and extensometers, each with three repetitions – is 6.26 Msi (43.2 GPa) with a CoV of 17%, as reported at the end of Table 1. For stiffness-critical secondary airframe components, such as fittings and gussets, which typically transfer load between primary components via mechanical fastening and exhibit complex 3D geometries, this material form seems to be most appealing. However, it also poses new challenges for the aerospace world, such as measuring and estimating the elastic response of a part, or predicting the location of peak stress and failure in a part containing a hole. Future work will be aimed at correlating the non-homogenous nature of the material sub-structure with ultrasonic inspections and DIC modulus measurements.

CONCLUSIONS

Experiments show that this form of discontinuous fiber composite specimens, obtained by slitting and chopping carbon fiber/epoxy prepreg tape, exhibit high surface strain variations, both across the width and along the length of a typical tensile specimen. These in turn lead to variation in modulus measurements by as much as 50% and a CoV of variation as high as 17%. It is not recommended to measure the modulus as with typical continuous fiber composites by applying a couple of back-to-back strain gages in the center of the specimen, or placing an extensometer on one side of the specimen. Longer strain gages do not appear to yield better results than shorter gages, and extensometer readings are not necessarily better than strain gage ones. The DIC technique has shown to give great insights in the behavior of the specimen, which is characterized by a highly non-homogenous substructure, and provide the most comprehensive modulus measurement by averaging the full-field strain values.

ACKNOWLEDGMENTS

The authors wish to acknowledge Dr Alan Miller (Director, Boeing 787 Technology Integration) for supporting this study. The contributions throughout the project of Dr. John Halpin are also gratefully acknowledged. The technical discussions with Prof C. T. Sun, Prof Byron Pipes, and Prof Ken Riefsnider have contributed to strengthening this paper. For the DIC technique, the authors would like to thank Mr Jon James of Correlated Solutions Inc. The authors would also like to thank undergraduate Enrique 'Gally' Galgana.

REFERENCES

1. Miller, A.G. (2007). The Boeing 787 Dreamliner, Keynote Address, In: *48th AIAA/ASME/ASCE/AHS/ASC Structures, Structural Dynamics, and Materials Conference*, Waikiki, HI.
2. Stickler, P.B. (2002). Composite Materials for Commercial Transport – Issues and Future Research Directions, In: *Proceedings of the ASC, 17th Annual Technical Conference*, West Lafayette, IN.
3. Halpin, J.C. (1969). Stiffness and Expansion Estimates for Oriented Short Fiber Composites, *Polymer Engineering and Science*, **3**: 732–734.
4. Halpin, J.C. and Pagano, N.J. (1969). The Laminate Approx. for Randomly Oriented Short Fiber Composites, *Polymer Engineering and Science*, **3**: 720.
5. Halpin, J.C. and Kardos, J.L. (1978). Strength of Discontinuous Reinforced Composites, *Polymer Engineering and Science*, **18**(6): 496–504.
6. Kardos, J.L., Michno, M.J. and Duffy, T.A. (1974). Investigation of High Performance Short Fiber Reinforced Plastics, Final Report, Naval Air Systems Command, No. N00019-73-C-0358.
7. Porter, J. (2004). Moving Closer to the Goal of Cost Effective Complex Geometry Carbon Composite Parts, HPC4HPC Special Session, In: *Proceedings of the 19th ASC Technical Conference*, Atlanta, GA.
8. Boeing 787 Features Composite Window Frames, Reinforced Plastics, *Application News*, **51**(3): 4.
9. Feraboli, P., Peitso, E., Deleo, F., Cleveland, T. and Stickler, P. (2009). Characterization of Prepreg-based Discontinuous Carbon Fiber/Epoxy Systems: Part I, *Journal of Reinforced Plastics and Composites*, **28**(10): 1191–1214.
10. Feraboli, P., Peitso, E., Cleveland, T., Stickler, P. and Halpin, J. (2009). Notched Behavior of Prepreg-based Discontinuous Carbon Fiber/Epoxy Systems, *Composites (Part A)*, **40**(3): 289–299.
11. Boeing standard test method for unnotched tension, D6-83079-61, The Boeing Co.
12. McGowan, D.M., Ambur, D.R., Hanna, T.G. and McNeill, S.R. (1999). Evaluation of the Compressive Response of Notched Composite Panels Using a Full-Field Displacement Measurement System, In: *40th AIAA Structures, Structural Dynamics and Materials Conference*, St. Louis, MO, No. 99-1406.
13. Feraboli, P. (2006). Damage Resistance Characteristics of Thick-core Honeycomb Composite Panels, In: *47th AIAA/ASME/ASCE/AHS/ASC Structures, Dynamics and Materials Conference*, No. 2006-2169, Newport, RI.
14. Harper, L.T., Turner, T.A., Warrior, N.A. and Rudd, C.D. (2006). Characterization of Random Carbon Fibre Composites from a Directed Fibre Preforming Process: The Effect of Fibre Length, *Composites Part A*, **37**(11): 1863–1878.
15. Harper, L.T., Turner, T.A., Warrior, N.A., Dahl, J.S. and Rudd, C.D. Characterisation of Random Carbon Fibre Composites from a Directed Fibre Preforming Process: Analysis of Microstructural Parameters, *Composites Part A*, **37**(11): 2136–2147.